Geoacoustic Model Parameter Estimation Using a Bottom Moored Hydrophone Array

R.M.S. Barlee, M.J. Wilmut, and N. R. Chapman

School of Earth and Ocean Sciences

University of Victoria,

Victoria, BC, Canada, V8W 3P6

Abstract—**This paper describes results from an experiment carried out to investigate geoacoustic inversion with a bottom moored hydrophone array located in the shallow waters of the Timor Sea off the northern coast of Australia. The array consisted of two arms in a V-shape, horizontally moored to a bottom was essentially flat over a large area. Hydrophone positions were estimated using an array element localization technique. The data used for geoacoustic inversion were from four tones in the 80 - 195 Hz band. A hybrid search algorithm determined the set of geoacoustic model parameters that maximized the Bartlett fit (averaged coherently spatially at each tone and incoherently over frequency) between the measured and modelled data at the array. The inverted geoacoustic profile performed well in a simple test for localizing the sound source at other sites in the vicinity of the array.**

Index Terms— **Inversion, geoacoustic, localization.**

I. Introduction

Knowledge of the ocean bottom is an essential component in modeling sound propagation in shallow water. Matched-field inversion (MFI) [1,2] estimates the parameters of geoacoustic models by matching measured field data with modeled data. The model providing one the best fit to the data is taken as an estimate of the true model parameters. Most experiments to date have performed MFI using data from vertical line arrays (VLA). However these arrays are expensive to build, deploy and maintain. As well, it is difficult to determine and monitor their array element positions, a crucial requirement for successful MFI. A VLA can only determine a source's range and depth unless environmental symmetry breaking is present; whereas horizontal line arrays have the potential for three dimensional source localization. This paper describes geoacoustic inversion of data obtained from a bottom moored horizontal array.

In November 1998, a sea trial to evaluate rapidly deployable array systems called RDS-2 was conducted in the Timor Sea off the north coast of Australia [3]. One of the experiment's objectives was to study the effectiveness of advanced signal processing applications using data obtained from rapidly deployable systems (RDS) in shallow water environments.

In this paper we examine geoacoustic inversion using the rapidly deployable, cost effective, autonomous, bottom moored ULITE array [3]. This array has three identical 470 m long arms extending from a central node. Each arm has 32 elements in three distinct nests with nest spacing 7.8 m, 15.6 m and 31.3 m. The deployment plan called for the array arms to be fully deployed with the arms separated by 120 degrees. The planned and deployed array positions can be seen in Fig. 1.

This paper describes the inversion method and presents results in determining geoacoustic parameters at the RDS-2 site. First, the crucial preliminary step of array element localization (AEL) is discussed in section II. Next, in section III, an effective hybrid search algorithm is described and applied in an inversion based on matched field processing to determine the geoacoustic parameters for a range independent geoacoustic model. One output of the algorithm is a measure of the relative sensitivities of these parameters. Section IV then evaluates the estimated geoacoustic model by using it in the localization of an acoustic source by the ULITE array. Finally, conclusions are presented in Section V.

II. Array Element Localization

A. AEL Method

Because the ULITE array was deployed by vessels on the surface and then dropped to the seafloor, factors such as surface winds, ship drift and subsurface currents all conspired to produce large uncertainties not only in the positions of individual hydrophones, but in the entire array itself.

Receiver location errors have been shown to lead to significant degradation of MFP performance [2], especially at higher frequencies (a commonly accepted rule suggests receiver positions must be known within λ/10, where λ is the wavelength at the frequency of interest, to achieve losses ≤1 dB in array processing [1]). As such, accurate array element location (AEL) is an important component of effectively processing acoustic field data.

For this experiment, AEL is conducted by inverting arrival times of transient pulses recorded by the array. First, light bulbs are imploded under the surface at various locations around the approximate array position. The implosion transients are recorded and the direct path pulse is up-sampled and fit to a parabola to determine the relative arrival times each hydrophone. Determining source (bulb) and receiver (hydrophone) positions from the relative arrival times presents an ill-posed inverse problem that is solved using regularized linear inversion [4,5]. The method yields the smoothest array shape (i.e., the shape with minimal curvature or changes in direction) that fits the acoustic data and a priori position estimates to a statistically appropriate level. This minimum-structure solution includes all array-shape structure that is resolved by the data, but no structure that is unconstrained. Additionally, unlike other methods that employ forward calculations to calculate blanket uncertainty estimates, linearized inversion provides precise uncertainty estimates for each hydrophone position.

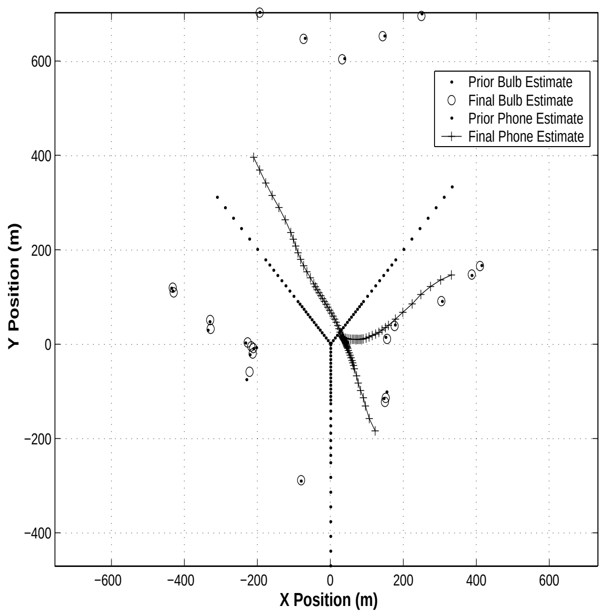

Fig. 1. Prior and final position estimates for hydrophones and bulb implosions used in array element localization of ULITE array.

B. AEL Results

Figure 1 depicts the intended (a priori) and estimated hydrophone positions of the ULITE array. Significant differences are apparent, with prior position residuals (the difference between intended and estimated positions) averaging 40 m in x and 88 m in y.

Uncertainties in hydrophone positions are calculated using 50 realizations of a Monte Carlo appraisal of the estimated positions [5]. Standard deviations of relative uncertainties average 50 cm in the x and y directions and 60 cm vertically, which corresponds to approximately $\lambda/14$ at 195 Hz, the highest frequency used in the analysis below.

III. GEOACOUSTIC INVERSION

C. Inversion Algorithm

In matched-field inversion we seek to find the minimum of an objective function E(m) where m is a set of geometric and geoacoustic model parameters. This function measures the mismatch between the measured data from an array of hydrophones and the modeled replica fields, the set of geoacoustic model parameters associated with the minimum defines the environment. This is a challenging problem as the multidimensional search space has many local minima, correlated variables, and variables with different sensitivities.

The 1997 Geoacoustic Inversion Workshop was held to compare various inversion techniques for a number of geoacoustic inversion test cases [6]. We use in this work, a hybrid algorithm, adaptive simplex simulated annealing (ASSA), that is shown to generate the best overall results for the workshop test cases detailed in ref. [7]. ASSA combines the well known global random search method, simulated annealing [SA], and a local gradient based directed search method, downhill simplex (DHS). SA is made up of a series of random perturbations of the model parameters. Perturbations that decrease the energy are always accepted while those that increase the energy are accepted with probability

$$P(\Delta E) = e^{-\Delta E/T} \tag{3.1}$$

where ΔE is the change in energy and T (temperature) is a control parameter. Accepting perturbations that increase E means that the algorithm can escape from local minima. High values of T allow escape from local minima with high probability, as T decreases this probability becomes smaller. The temperature is slowly reduced as the algorithm proceeds. The form of the temperature reduction schedule, while problem specific, is not too difficult to determine. It is the algorithm's main control parameter. DHS is a procedure that yields a downhill step (model with lower energy) without evaluating partial derivatives or solving systems of equations. The procedure uses a simplex of N+1 models to navigate the N (the number of model parameters) dimensional search space. ASSA generates an initial random simplex. Subsequent changes to the simplex consist of a DHS step and a random perturbation of the trial model that is accepted or rejected according to the SA criteria. Unlike SA the algorithm retains the best model (lowest energy) found to date. The parameter perturbation search sizes are set adaptively based on the running average of accepted perturbations, rather than the arbitrary temperature schedule. The evolving simplex allows the algorithm to avoid local minima, navigate the narrow valleys in the search space due to correlated parameters, and search more effectively in the region of the global minimum. The result is an efficient, effective, easy to use search algorithm.

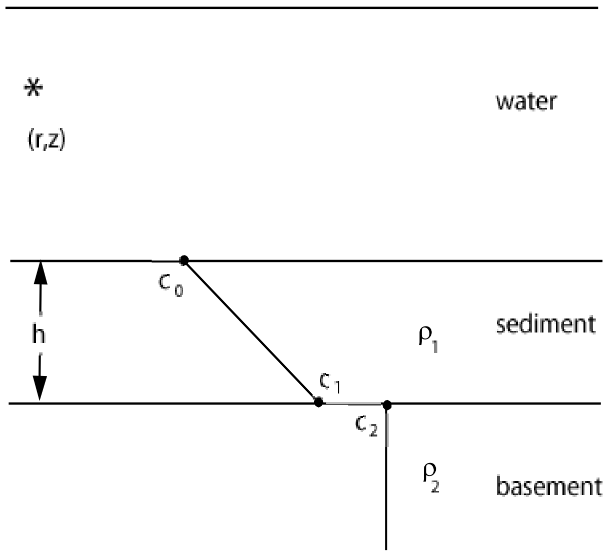

Fig. 2. Geoacoustic model denoting parameters of interest

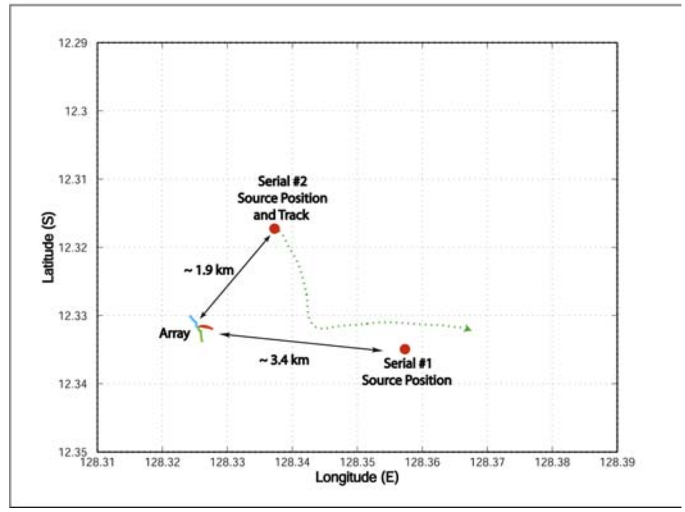

Fig. 3. Geometric setup of acoustic serials considered in this paper

D. *Inversion of RDS-2 Data*

The bathymetry in the vicinity of the trial site indicates an extensive flat bottom of 107 m depth. Using a priori knowledge based on historical geoacoustic data for the trial region, a range independent two layer over a half space model is assumed for the site. The six unknown geoacoustic parameters sought are sediment thickness (*h*), sound speed at the top of the sediment layer (c_0), sound speed at the bottom of the sediment layer (c_1), sound speed in the basement (c_2), and the densities in the sediment (ρ_1), and in the basement (ρ_2). These parameters are shown in Fig. 2. The sound speed profile in the water layer was measured during the experiment. A normal mode propagation model ORCA [8] is used to calculate the replica vectors for the environment.

Data for geoacoustic inversion was collected during an 'all quiet' ship state known here as *serial 1*. The source projector was suspended from a stationary ship bearing 096 true at 3.4 km from the array node at a depth of 55m. Six low frequency tonals between 80 and 225 Hz were emitted from the projector with the per sensor SNR greater than 20 dB at each frequency. The data recorded from the NW and NE arms of the array (a V shaped array) at 80, 95, 125 and 195 Hz. are used for the inversion. Fig. 3 depicts the serial geometry.

The objective function, or energy *E*(*m*), is one minus the Barlett processor averaged over NF = 4 frequencies as follows,

$$E(m) = 1 - \frac{1}{NF}\sum_{i=1}^{NF} \left| \sum_{j=1}^{NH} P_j P^{*}{}_j(m) \right|^2 \qquad (3\ .2)$$

where P_j is the measured complex pressure field and $P_j(m)$ is the modeled pressure field for model *m*, both of which have dimension *NH,* the number of hydrophones, and unit magnitude.

There were nine unknown parameters in the search, the six geoacoustic noted above and three geometric (the search was conducted in a small window about the nominal source location). The parameter search limits can be found in Fig. 4. ASSA was run using 1000 temperature steps, an initial temperature of 0.3 and a reduction factor of 0.997. The energy and accepted parameter estimates are plotted in Fig. 4 as a function of the temperature step. The objective function minimum was 0.34. It can be seen that the sediment thickness and sound speed estimates converged before the density estimates. This sequential converging is due to the adaptive setting of each individual parameter perturbation search size. This feature of the algorithm allows more intense searching in the region containing the global minimum for each parameter.

Fig. 5 is a plot of energy as a function of the parameter values, where the dotted line indicates the parameter value with the lowest energy. This is a useful way to display parameter sensitivity. A sensitive parameter is one for which a small change in the parameter value, near the minimum, results in a large change in the energy. It can be seen that the most sensitive parameters are sediment thickness and sound speeds in the sediment, sound speed in the basement is somewhat sensitive and the densities are relatively insensitive. Additionally, when examining the geometric parameters, the bearing shows highest sensitivity, followed by depth, and finally range.

IV. Source Localizatioin

Traditionally, reliability of geoacoustic inversion parameter estimates is assessed against ground truth data. Here, we propose assessing the accuracy or effectiveness of the estimated geoacoustic model, by using it in 3-D localization of an acoustic source at the RDS-2 site. Two situations are considered. First, localization is attempted for the four-tone source placed at the same location as the inversion (serial 1), but a few seconds later.

The results are shown in Fig. 6. Here, averaged Bartlett processor output is plotted as a function of search range and

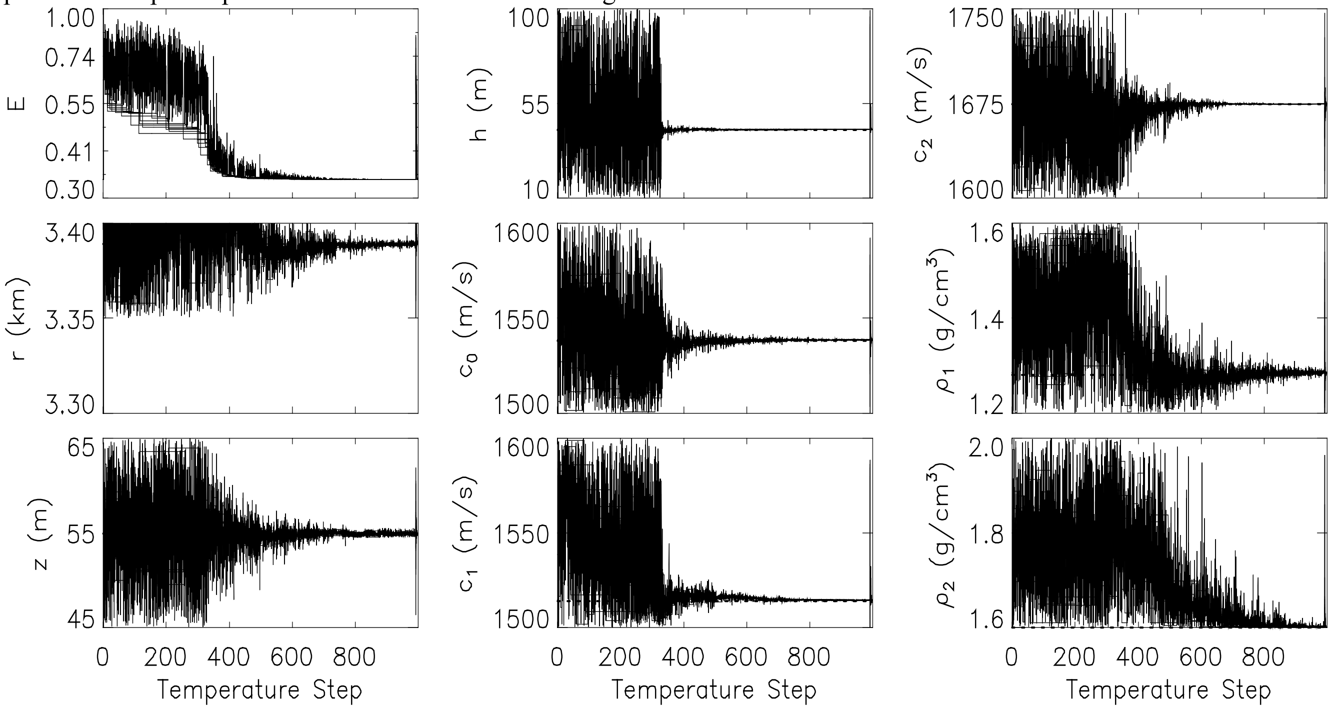

Fig. 4. Energy , *E(m),* and parameter estimates vs. temperature step from ASSA inversion. Dotted lines indicate parameter estimates associated with lowest energy.

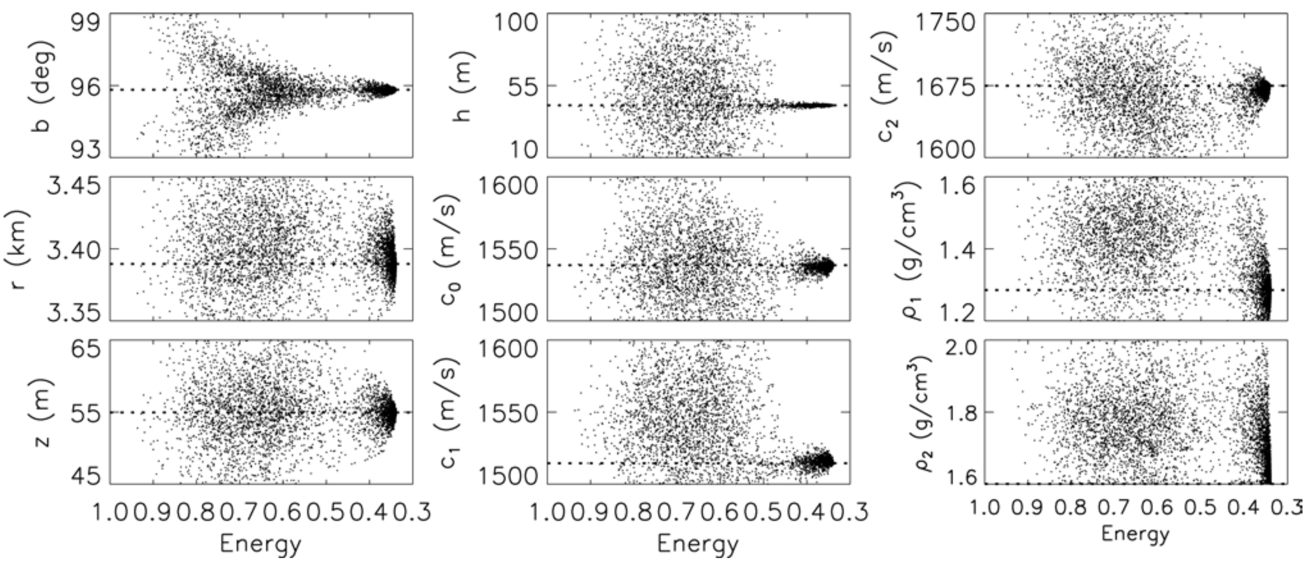

Fig. 5. Energy (dots) plotted as a function of parameter values. Dotted lines indicate parameter estimates associated with lowest energy.

bearing for the depths noted in each window. Not surprisingly, the maximum Bartlett averaged value is at the true source location with a value of 0.66. This peak is 5.47 standard deviations above the mean background with excellent range, bearing and depth resolution. The sidelobes are well below the main peak. This result suggests that the environment is sufficiently well modeled to allow the array to localize the four-tone source.

In the second scenario localization is attempted when the tow ship was 1.9 km from the array node at bearing 041 true. The projector was towed approximately 100 m behind the ship (steaming at 3-4 kn with a keel depth of 6m) at a depth of 54 m. Fig. 3 depicts the geometry, labeled *serial 2*. Here only two projector tonals were emitted at 80 and 110 Hz, and because of severe signal interference from ship noise, localization was not possible due to strong sidelobes on the ambiguity surface. Consequently, three stable ship frequencies (25, 38, 79 Hz) were included in the MFL to increase localization performance. Fig. 7 depicts the associated spectrum. The resulting ambiguity surface (not shown) indicates a Bartlett average maximum of 0.55, obtained at a depth of 6m (consistent with the tow ship depth), range of

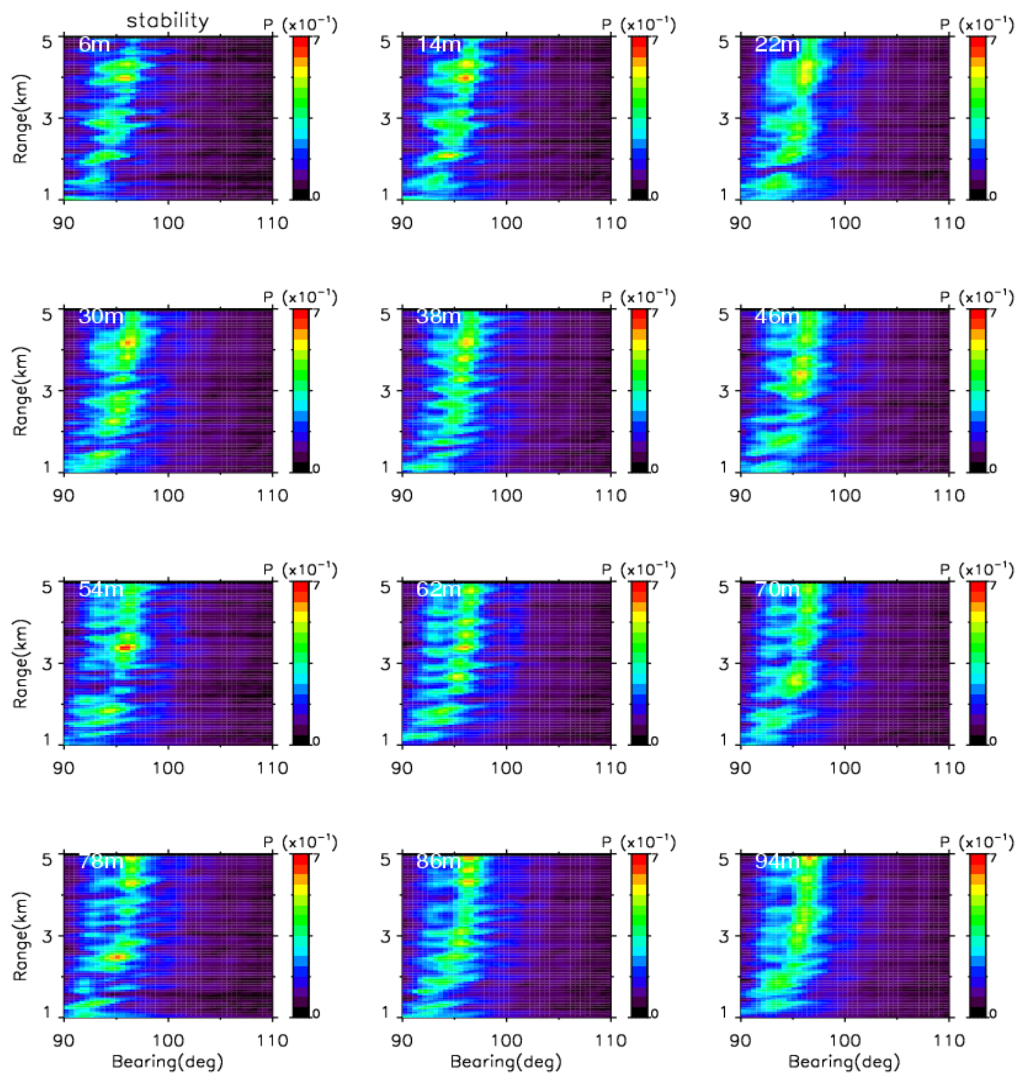

Fig. 6. Averaged Bartlett Processor output as a function of search range and bearing for the set of 12 noted depths.

1.725 km and bearing of 041 true. The peak is 3.1 standard deviations above the mean background level and is discernable from sidelobes. These results from the two localization scenarios suggest that assumption of a range independent geoacoustic environment is adequate for the site.

V. CONCLUSION

A geoacoustic model is obtained by matched field inversion of bottom moored horizontal array data for the shallow water site of the RDS-2 experiment in the Timor Sea. The ASSA inversion algorithm gives not only parameter estimates but also parameter sensitivities. The geoacoustic model provides an effective approximation to the environment allowing 3D source localization. The first scenario used the same source position and frequencies but a different time for localization, while the second used a different position, frequencies and time. The results suggest the derived geoacoustic model well describes a portion of the RDS-2 experimental region over a set of frequencies. This analysis could be expanded into a systematic approach to more fully determine the validity of the range independent assumption and the robustness of the model for sound frequencies not used during the inversion. An inversion/localization experiment is suggested that would consist of fixed range inversions (using a projector emitting a set of frequencies) carried out at a set of gridded positions in the area of interest. A set of possibly location dependent geoacoustic models would be obtained. The projector (emitting the frequencies used for inversion, plus other frequencies) would then be towed between the positions at which the inversions were done. One could then determine the range variability by examining how well the geoacoustic parameter set from one location localizes a source at other positions and frequencies.

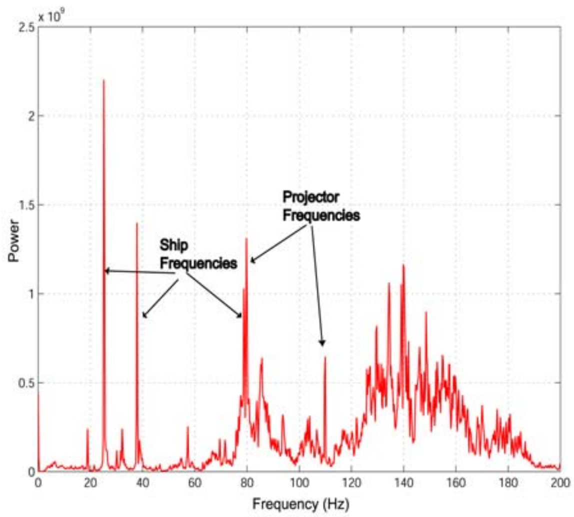

Fig. 7. Serial 2 average spectrum over 24 sec window.

Acknowledgments

Research supported by funding from a Natural Sciences and Engineering Research Council partnership peogram with General Dynamics Canada and the Canadian Department of National Defense.

References

[1] A. Tolstoy, *Matched-field Processing for Underwater Acoustics*, World Scientific, 1993.
[2] A. B. Baggeroer, W.A. Kupperman, and P.N. Mikhalevsky, "An overview of matched field methods in ocean acoustics," *IEEE J. Ocean Eng.*, vol. 18, no. 4, pp. 401-423, 1993.
[3] Rapidly Deployable Systems TTCP Trial RDS-2: Joint Trial Plan, DSTO Australia, October 1998.
[4] S.E. Dosso, M.R. Fallat, B.J. Sotirin, and J..L. Newton, "Array element localization for horizontal arrays via Occam's inversion," *J. Acoust. Soc. Am.*, vol. 104, pp. 846-859, 1998.
[5] R.M.S. Barlee, S.E. Dosso, and P. Schey, "Array Element Localization of a Bottom Mounted Hydrophone Array", *Cdn. Acoustics.*, vol. 30, no. 4, pp. 3-12, 2002.
[6] A. Tolstoy, N.R. Chapman, and G.H. Brooke, "Benchmarking geoacoustic inversion methods", *J. Comput. Acoust.*, vol. 6, no. 1-2, pp. 1-28, 1998.
[7] S.E. Dosso, M.J. Wilmut, and A.S. Lapinski, "Adaptive-Hybrid algorithm for geoacoustic inversion", *IEEE J. Ocean Eng.*, vol. 26, no. 3, pp. 324-336, 2001.
[8] E. K. Westwood, C. T. Tindle, and N. R. Chapman, "A normal mode model for acousto-elastic ocean environments", *J. Acoust. Soc. Am.*, vol. 100, no. 6, pp. 3631-3645, 1996.